Attractor dynamics drive flexible timing in birdsong

Fjola Hyseni, Nicolas P. Rougier, Arthur Leblois

Attractor dynamics drive flexible timing in birdsong

Fjola Hyseni[1,2][0000−0001−5533−2270], Nicolas P. Rougier[1,2,3][0000−0002−6972−589X], and Arthur Leblois[1][0000−0002−9392−5939]

[1] CNRS, IMN, UMR 5293, F-33000, Bordeaux, France,
[2] LaBRI, Université de Bordeaux, Talence, France
[3] Inria Bordeaux Sud-Ouest, Talence, France

Abstract. Timing is a critical component of a wide range of sensorimotor tasks that can span from a few milliseconds up to several minutes. While it is assumed that there exist several distributed systems that are dedicated for production and perception [1], the neuronal mechanisms underlying precise timing remain unclear. Here, we are interested in the neural mechanisms of sub-second timing with millisecond precision. To this end, we study the control of song timing in male Zebra Finches whose song production relies on the tight coordination of vocal muscles. There, the premotor nucleus HVC (proper name) is responsible for the precise control of timing. Current models of HVC rely on the synfire chain, a pure feed-forward network. However, synfire chains are fragile regarding noise and are only functional for a narrow range of feed-forward weights, requiring fine tuning during learning. In the present work, we propose that HVC can be modelled using a ring attractor model [2], where recurrent connections allow the formation of an activity bump that remains stable across a wide range of weights and different levels of noise. In the case of asymmetrical connectivity, the bump of activity can "move" across the network, hence providing precise timing. We explore the plasticity of syllable duration in this framework using a reward-driven learning paradigm and a reward-modulated covariance learning rule applied to the network's synaptic weights [3]. We show that the change in duration induced by the learning paradigm is specific to the target syllable, consistent with experimental data.

Keywords: Timing · Songbirds · Attractor.

1 Introduction

Timing is crucial for a wide range of sensorimotor tasks. However, there are numerous uncertainties regarding the underlying mechanisms. For instance, sensory and motor timing may or may not rely on the same circuitry, there could be different mechanisms for different scales of timing (subsecond, suprasecond etc.) and it can be considered as a dedicated or intrinsic system [4] [5]. In this study, we focus on motor timing at the scale of tens to hundreds of milliseconds. Addressing this question has led to the design of several computational models such

as ramping models, internal clocks, population clocks, labeled-line models and multiple-oscillator models [6, 7]. Ramping model-like patterns of activity during timing tasks [8–10] have been observed in multiple brain areas, but it is unclear whether they are indeed timekeepers or whether they reflect motor preparation instead. On the other hand, internal clocks provide a linear readout of time, assuming the presence of a pacemaker-integrator system, the location of which remains unclear[7]. Lastly, population clock models assume that time is encoded in the dynamically changing population of neurons, but have the limitation of lacking an intrinsic metric of time. They are, however, well suited for pattern timing underlying speech and birdsong.

Birdsong relies on the tight coordination of vocal muscles with a precise timing at the scale of tens to hundreds of milliseconds. In songbirds, a localized timing area has been identified in the premotor nucleus HVC (proper name). HVC projects to a downstream motor nucleus controlling syringeal and respiratory muscles. Neurons in HVC projecting to downstream motor nucleus fire in a time-locked manner during singing, producing a single 10 ms long burst of 3-6 spikes [11]. Manipulating HVC temperature modifies song duration, with a dilation and song stretching when HVC is cooled [12], supporting the hypothesis of HVC as a population clock model.

The dynamics of neuronal activity in the nucleus HVC of songbirds have been previously modelled with networks of excitatory neurons organized in a sequentially connected chain of neuronal populations, referred to as *synfire chain* [13], belonging to the class of population clocks. However, the purely feedforwad connectivity pattern of synfire chains does not appear compatible with the connectivity patterns revealed experimentally in cortical networks. More specifically, unidirectional connectivity between groups of neurons is incompatible with the high level of reciprocal connectivity typically observed in cortex [14]. Additionally, synfire chain networks are sensitive to noise and not very robust to weight variability, requiring very precisely tuned synaptic strengths to avoid runaway excitation or decay.

An alternative hypothesis is that the gradual propagation of an activity bump is driven in HVC by attractor dynamics. In particular, a linear attractor, also referred to as ring attractor, can drive a drifting activity bump with robust and resilient properties thanks to recurrent connections [2]. However, it remains unclear if the ring attractor can account for the properties of HVC neuronal dynamics and the behavioral adaptation of song timing. In previous studies [15, 16], timing flexibility in motor timing in adult songbirds has been investigated, through targeting a syllable for modification using a Conditional Auditory Feedback (CAF) protocol (based on reinforcement learning). The results showed that birds can change the targeted element of their stereotyped song with specificity, i.e. with no effect on other syllables. Upon confrontation of these results with three modelling approaches, only synfire chains and not attractors, could account for specificity in adaptive learning. Conversely, we propose and provide evidence that a structured attractor, such as the ring attractor, can simulate adaptive learning and provide results consistent with behavioral data.

2 Methods

2.1 Ring Attractor

We first consider a neural population of 1000 units whose mean firing rate is expressed as $m(x,t)$ with x being the position over a closed one-dimensional manifold (ring) and t represents time. The evolution of $m(x,t)$ is governed by equation:

$$\tau \frac{d}{dt} m(x,t) = -m(x,t) + G(I_{ext}(x,t) + I_{syn}(x,t) - T + \sqrt{\tau_n}\sigma_n \eta(x,t)), \quad (1)$$

where τ is the neuronal membrane time constant. On the right hand side (rhs) of Eq. (1), I_{ext} is the external constant input, I_{syn} the synaptic input and T represents the threshold. The last rhs term is a zero-mean Gaussian white noise. For the nonlinear gain function $G(I)$, the simple semi-linear form is adopted:

$$G(I) = \begin{cases} 0 & I < 0 \\ I & 0 < \quad I < 1 \\ 1 & I > 1 \end{cases} \quad (2)$$

We use the following expression for the synaptic input:

$$I_{syn}(x,t) = \sum_{x'=1}^{N} \frac{1}{N} W(x - x') m(x', t), \quad (3)$$

where $\sum_{x'=1}^{N}$ denotes a summation over all neuronal indices. The weight matrix W is choosen of the following form:

$$W(x - x') = W_0 + W_2 \frac{1}{\sigma\sqrt{2\pi}} e^{-\left(\frac{x-x'+\beta}{2\sigma}\right)^2}, \quad (4)$$

where W is defined based on the neurons' preferred timing (see Fig. 1 (A)) and not on the spatial topology, as HVC microcircuitry does not display spatio-temporal organization (see Fig. 1 (B)). The parameter W_0 stands for the global inhibition, W_2 the excitation factor, σ the standard deviation and β is the bias term which makes the connectivity pattern asymmetric.

2.2 Implementing a Reward-Covariance Reinforcement Learning Rule

Equations of the learning rule are implemented based on a reward-covariance learning rule [3], to adaptively change W:

$$\Delta W_{ij} = \gamma R e_{ij} \qquad \text{with} \quad e_{ij} = \int_0^t \frac{dt'}{\tau_e} e^{-(t-t')/\tau_e} \eta_i(t') m_j(t'), \quad (5)$$

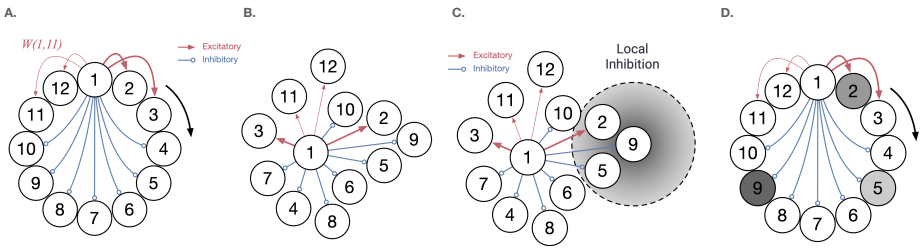

Fig. 1: **Simplified illustration of the ring connectivity and consequences of local inhibition.** (A) The connectivity is represented using the preferred timing as a neighbourhood proxy for the placement of neurons. (B) The same connectivity is represented using the physical location of neurons. (C) Injection of a local inhibition in nucleus HVC. (D) The same local inhibition shown when neurons are ordered according to their preferred timing. In this spatial representation, the effect is not local, but rather distributed, which makes the network more robust.

j and i represent the pre- and postsynaptic neurons, respectively. The learning rateγ is chosen to match learning rates observed in songbirds experiments, R the reward value and e_{ij} the eligibility trace, τ_e is the eligibility time constant, η_i the noise of the postsynaptic and m_j the rate of the presynaptic neuron. R takes a value of 0 or 1, when the syllable is targeted for modification and 0 when it is not. At the end of each learning trial, a reward of 1 is given if the targeted syllable duration is lower (higher) than the updated target duration. This paradigm is based on the one introduced in [16], where $I^{(tar)}$ denotes the current duration of the syllable, and $\bar{I}^{(tar)}$ represents the running average of the target syllable duration, which is updated after every trial according to the following:

$$\bar{I}^{(\mathrm{tar})} \leftarrow 0.995\bar{I}^{(\mathrm{tar})} + 0.005I^{(tar)}, \tag{6}$$

across the 1000 learning trials. Additionally, prior to learning, we run 50 trials with no reinforcement to determine a baseline distribution of syllables. Following learning, we run 50 more trials without reinforcement and with the updated weight matrix W ($W_{initial} + \Delta W$). Significant change between these two duration distributions is determined by performing independent t-tests.

2.3 Analysis

The quality of the model is evaluated regarding several objectives.

- The speed of the bump, which acts as a proxy for the accuracy of the timing,
- the mean syllable duration when noise is present, and
- the capacity for the model to shorten or lengthen a syllable duration without interferring with others.

Bump speed At any time, the position $C(t)$ of the bump of activity can be measured using the center of mass (COM) of the whole population, based on equations for COM in systems with periodic boundary conditions. This center $C(t)$ is further discretized into $\bar{C}(t)$ such as to coincide with the nearest unit position:

$$\bar{C}(t) = argmin_i(C(t) - x_i). \tag{7}$$

The speed of the bump is then computed as the displacement (in the neuronal feature space) of the center of mass over time.

Syllable definition and duration A syllable corresponds to a fixed segment of the ring. Mean syllable length in zebra finches has been reported to be 110 ± 56 ms [17]. We choose a syllable duration close to the mean reported value and for simplification, we chose equal size segments such that for s syllables and n neurons, syllable i is defined by $[\frac{i}{s}n, \frac{i+1}{s}n]$. Syllable duration is then measured from when the center of the activity bump $\hat{C}(t)$ crossed the lower limit of the segment up to when it crossed the upper limit of the segment.

Simulation All simulations were performed using Euler integration with a timestep (dt) of 0.25 ms. Multiple runs were performed to identify an appropriate (high enough) value for dt that does not alter the outcome. Parameter values for the simulations are detailed in Table 1.

Table 1: Values of the parameters used in Eqs.(1) - (5).

Parameters	Values	Parameters	Values
N (number of neurons)	1000	T (threshold)	0.9
dt (timestep)	0.25 ms	W_0	-5
duration	2 s	W_2	7
τ (membrane time constant)	10 ms	β (bias in the weight matrix)	0.05 radians
I_{ext} (external constant input)	1.1	σ (Eq. (4))	0.067
τ_{noise} (time constant of the noise)	1 ms	σ_{noise}	0.01
γ (learning rate)	0.004	τ_e (eligibility trace time constant)	35 ms

3 Results

In the ring attractor model, recurrent connections allow for the formation of an activity bump that remains stable across a wide range of weights. In the presence of a fully symmetric connectivity and a constant stimulus, the activity bump settles in one of the stationary states and remains there until another input or a high enough perturbation is exerted. However, since the purpose of this model is to generate a sequential activity, we investigate how propagation across these states can be achieved.

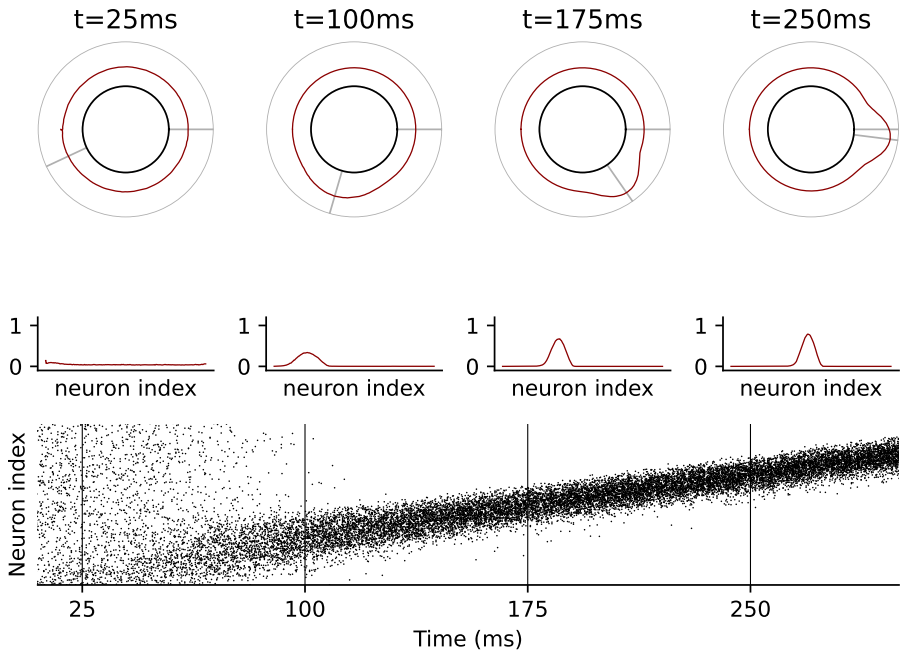

Fig. 2: **Activity propagation in the ring.** The first two panels show the position of the bump of activity (normalized firing rate) in the network at a particular point in time. The third panel serves to present the possible spiking pattern this rate network would be compatible with. They were generated using a homogenous Poisson process.

3.1 Moving Bump

Three ways to ensure bump propagation have been identified. These include an external drive in the form of a moving stimulus, adaptation and an asymmetric connectivity profile. In the case of a moving stimulus, the velocity/speed of this stimulus has a linear relationship with the speed of the bump.

Intrinsic drive: Adaptation and Bias Adaptation [2] can make the bump move by generating a local, strong, delayed negative feedback, and hence suppressing localized activity. This causes higher activity in the nearby unadapted region. Moreover, making the connectivity pattern asymmetric by adding a bias also ensures bump propagation. The activity bump's center of mass encodes time such that at time $t(x)$, neuron x is maximally activated and as it moves across the network different neurons will be more active at different points in time (Fig. 2). The magnitude of the bias also exhibits a quasi-linear relationship with bump speed, such as the higher the bias, which assures the feedforwardness

of the network, the higher the speed of movement of the bump (Fig. 3). The rest of the presented results is for the asymmetric connectivity profile.

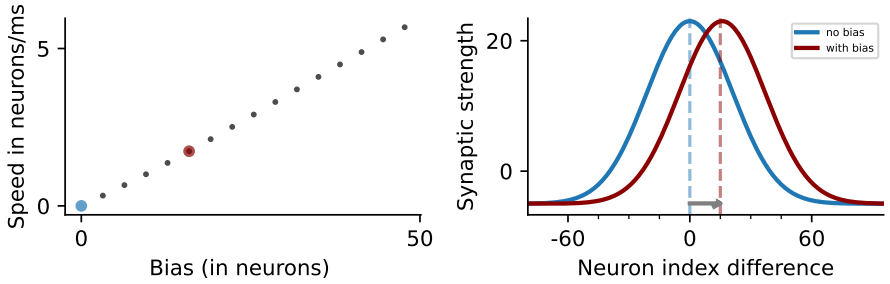

Fig. 3: **An asymmetric connectivity pattern makes the bump of activity move across the network.** (A) The speed of the bump is driven by the amplitude of the bias. This is a quasi-linear relationship. (B) Connectivity profile for each presynaptic neuron to the postsynaptic neurons with no bias and bias. (Neuron index difference = $presynaptic - postsynaptic$) This bias is the one we use for the rest of the results presented. Self-connections are set to 0 but not illustrated in the figure.

3.2 Robustness

We design a test protocol to evaluate the robustness of the network under possible biological perturbations. We simulate the local injection of a drug inducing the inhibition of neuronal activity (e.g. Muscimol) with an effect that spreads spatially according to a Gaussian spatial distribution into the network, as shown in Fig. 1(C, D). The formula of diffusion of the inhibitory substance is that of a Gaussian distribution and it is added to the main equation as an external inhibitory input:

$$I_i = \alpha \frac{1}{\sigma\sqrt{2\pi}} e^{-\frac{1}{2}(\frac{x-\mu}{\sigma})^2}.$$

We test distributions with different spatial widths (σ) or amplitudes (α). We show that the perturbation is diminished across time and, if not too high, there is no disruption in sequence generation and the speed of the bump is conserved. This allows us to make a prediction for the HVC behavior in presence of such inhibition. More precisely, this would mimic inhibition with a GABA-A agonist, Muscimol in HVC and the prediction states that there will only be a delay in the initiation of the sequence (song), but no further disruption as shown in Fig. 4, meaning the timing accuracy would be sustained.

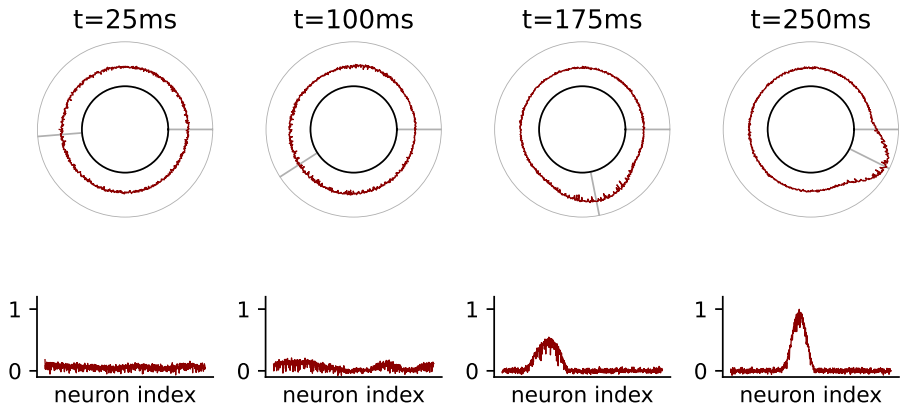

Fig. 4: **Influence of a local inhibition.** A local inhibition in the model (i.e. an inhibition that only affects a distributed sub-population) induces a delay in the initial formation of the bump even though the model can recover after tens of milliseconds. After this initial delay, the timing is correct.

3.3 Local Plasticity and Comparison with Experimental Data

To validate the model and to address the second question of whether the ring attractor is able to give account for experimental evidence witnessed in the CAF protocol [16], we use a reward covariance rule [3] for the conditioning. Consistent

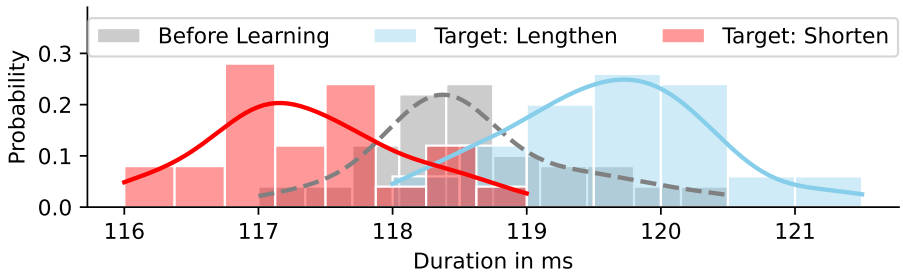

Fig. 5: **Syllable duration distribution before and after reinforcement learning (for decrease, increase) of the targeted syllable.**

with behavioral data, the duration of a syllable can be modified in response to a perturbed reward profile (Fig. 5) and this change is specific to the target syllable. No interference was present in adjacent or non-adjacent syllables, both in the case of targeting for a duration increase or decrease (Fig. 6).

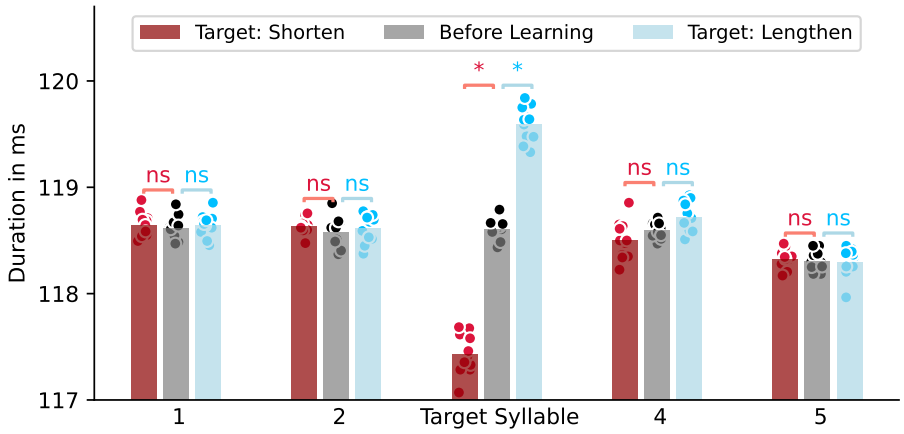

Fig. 6: **Adaptive learning is specific to the targeted syllables.** 10 runs (of 1000 trials) of learning, aiming to achieve syllable duration reduction (red)/ increase (blue) are run. Baseline mean duration is in gray. For each of the 10 runs in the three conditions, a mean duration is computed from the duration distribution; these are shown as points in the bar plot. Hence, the bars represent the mean duration across the 10 runs. * stands for $p < 0.001$. Only the target syllable is significantly affected after reinforcement learning.

The change in synaptic weights (ΔW), driving the change in syllable duration, is illustrated in Fig. 7. For instance, when the duration is targeted for shortening, connections from the presynaptic neurons to the postsynaptic neurons prior (neuron 450 to 500) are weakened and the ones to the postsynaptic ahead (neuron 500 to 550) are strengthened, changing slightly the slope of the bump and making it move faster in that area (defined by the presynaptic neurons).

4 Discussion and Conclusion

Attractor dynamics have been used to model a wide range of cognitive processes including memory representation, sequence generation, decision making, integration etc. [18]. A group of criteria have been proposed to claim possible attractor dynamics in different networks in the brain. HVC activity corresponds to the sequence generation category, and abides at least 4 out of 5 of these criteria, namely: i) Possession of a low-dimensional set of states that correspond to attractors in the state space (a one dimensional output in HVC) [11]. ii) Robustness to perturbation and return to the low-dimensional state after it. Electrical stimulation [19] in HVC perturbs song timing, but once removed, it is quickly restored. iii) Invariance and persistence of the states over time, in particular across states. In adult zebra finches, even in the absence of HVC main inputs

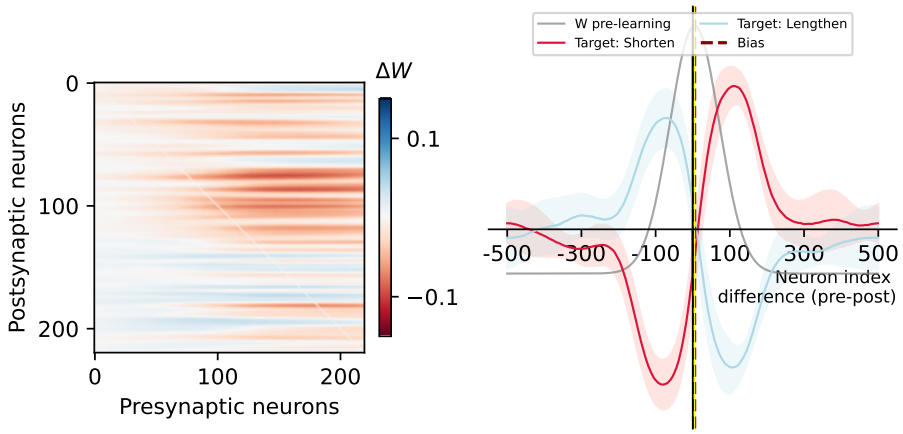

Fig. 7: **How do the weights change to achieve specific adaptive learning?** On the left: ΔW of a single run (target: decrease syllable duration), zoomed in at the area of pre and post-synaptic neurons encoding the target syllable. On the right: the change in synaptic weights across 10 runs of learning with respect to the presynaptic neurons encoding the target syllable, both when the target is reducing (red) the duration and increasing (blue) it. The thicker line represents the mean across runs and the filled in area the SD extracted from the means across the postsynaptic neurons of the ΔW for each of the 10 runs.

[20] [21], HVC neuronal activity underlying song production persists. Moreover, HVC singing-related activity can be evoked outside singing, e.g. during sleep [21]. iv) Isometry [22]. The fifth condition, pertaining to anatomical and structural correlates, remains to be studied and investigated further. However, there are three reasons that make us speculate it may be true as well. First, based on the resulting HVC dynamics, the underlying pattern could include reciprocal connectivity and relies on stronger connectivity between neurons firing at the same time in song. Secondly, as a local circuit encoding motor timing, HVC is expected to rely on regimes with strong internal connections capable of self-sustained activity [7]. Thirdly, evidence from mammalian visual cortex show that neurons with similar tuning, exhibit stronger connections.

As an attractor, the resulting model is robust to noise and weight variability. Moreover, it is compatible with HVC's sparse coding and exhibits specific learning, consistent with experimental findings. It is also able to derive an experimental predicition regarding possible neural dynamics in the HVC, in the presence of a local GABA-A agonist (Muscimol), which remain to be tested. However, the duration of the burst of activity observed in HVC in zebra finches (approx 10 ms) can only be reproduced with artificially short neuronal time constants (1 ms) in the rate model exposed here. For a more accurate representation of the spiking dynamics in the network and a short-duration burst of

activity spreading across the nucleus, it may be necessary to model the network with spiking neurons, e.g. using leaky integrators and relying on adaptation to minimize burst duration [23].

Some observations in the ring attractor lead to important questions in the songbird literature. For instance, activity propagation is possible not only through an asymmetric connectivity, but also adaptation, which is an intrinsic neuronal property. In this setting, we question whether the timing in birdsong is intrinsic (i.e coming from adaptation) or a combination of intrinsic and experience based factors (bias) [24] [25]. Furthermore, the connectivity pattern may be learned through sensory (auditory) stimulation of the nucleus during the sensory period of learning as HVC neurons can respond to auditory stimulation and may display mirror-like activity pattern during singing and auditory stimulation[26]. However, it still remains an open question.

Finally, songbirds are also known for being a good model for the neural mechanisms of vocal production in humans [27]. Therefore, similar neural mechanisms may underlie speech and song timing control. The dynamics of cortical neurons driving speech production may thus also be accurately represented by the present model.

References

1. Hazeltine, E., Helmuth, L.L., Ivry, R.B.: Neural mechanisms of timing. Trends in Cognitive Sciences **1**(5), 163–169 (Aug 1997). https://doi.org/10.1016/s1364-6613(97)01058-9
2. Hansel, D., Sompolinsky, H.: Modeling feature selectivity in local cortical circuits. Book Chapter (1998)
3. Williams, R.: Simple statistical gradient-following algorithms for connectionist reinforcement learning. Mach Learn (1992)
4. Robbe, D.: Lost in time: Rethinking duration estimation outside the brain. PsyArXiv. (2021). https://doi.org/10.31234/osf.io/3bcfy
5. Ivry, R., Schlerf, J.: Dedicated and intrinsic models of time perception. Trends Cogn Sci. **12(7)**, 273–80 (2008). https://doi.org/10.1016/j.tics.2008.04.002
6. Goel, A., Buonomano, D.V.: Timing as an intrinsic property of neural networks: evidence from in vivo and in vitro experiments. Philosophical Transactions of the Royal Society B: Biological Sciences **369**(1637), 20120460 (2014). https://doi.org/10.1098/rstb.2012.0460
7. Buonomano, D.V., Laje, R.: Population clocks: motor timing with neural dynamics. Trends in Cognitive Sciences **14**(12), 520–527 (Dec 2010). https://doi.org/10.1016/j.tics.2010.09.002
8. Durstewitz, D.: Self-organizing neural integrator predicts interval times through climbing activity. Journal of Neuroscience (2003). https://doi.org/10.1523/JNEUROSCI.23-12-05342
9. Simen, P., Balci, F., Souza, L., Cohen, J., Holmes, P.: A model of interval timing by neural integration. The Journal of neuroscience : the official journal of the Society for Neuroscience **31**, 9238–53 (06 2011). https://doi.org/10.1523/JNEUROSCI.3121-10.2011
10. Balci, F., Simen, P.: A decision model of timing. Current Opinion in Behavioral Sciences **8** (02 2016). https://doi.org/10.1016/j.cobeha.2016.02.002

11. Hahnloser, R., Kozhevnikov, A., Fee, M.: An ultra-sparse code underlies the generation of neural sequences in a songbird. Nature (2002). https://doi.org/10.1038/nature00974
12. Long, M., Jin, D., Fee, M.: Support for a synaptic chain model of neuronal sequence generation. Nature. 2010 Nov 18 (2010). https://doi.org/10.1038/nature09514
13. Jin, D., Ramazanoğlu, F., Seung, H.: Intrinsic bursting enhances the robustness of a neural network model of sequence generation by avian brain area hvc. J Comput Neurosci (2007)
14. Perin, R., Berger, T.K., Markram, H.: A synaptic organizing principle for cortical neuronal groups. PNAS (2011). https://doi.org/10.1073/pnas.1016051108
15. Ali, F., Otchy, T.M., Pehlevan, C., Fantana, A.L., Burak, Y., Ölveczky, B.P.: The basal ganglia is necessary for learning spectral, but not temporal, features of birdsong. Neuron **80**(2), 494–506 (Oct 2013). https://doi.org/10.1016/j.neuron.2013.07.049, https://doi.org/10.1016/j.neuron.2013.07.049
16. Pehlevan, C., Ali, F., Ölveczky, B.: Flexibility in motor timing constrains the topology and dynamics of pattern generator circuits. Nat Commun 9, 977 (2018). https://doi.org/10.1038/s41467-018-03261-5
17. Glaze, C.M., Troye, T.W.: Temporal structure in zebra finch song: Implications for motor coding. Journal of Neuroscience (2006). https://doi.org/10.1523/JNEUROSCI.3387-05.2006
18. Khona, M., Fiete, I.: Attractor and integrator networks in the brain. Nat Rev Neurosci **23**, 744–766 (2022). https://doi.org/10.1038/s41583-022-00642-0
19. Vu, E., Mazurek, M., Kuo, Y.: Identification of a forebrain motor programming network for the learned song of zebra finches. Journal of Neuroscience (1994). https://doi.org/10.1523/JNEUROSCI.14-11-06924.1994
20. Naie, K., Hahnloser, R.: Regulation of learned vocal behavior by an auditory motor cortical nucleus in juvenile zebra finches. J. Neurophysiol. (2011). https://doi.org/10.1152/jn.01035.2010
21. Elmaleh, M., Kranz, D., Asensio, A., Moll, F., Long, M.: Sleep replay reveals premotor circuit structure for a skilled behavior. Neuron (2021). https://doi.org/10.1016/j.neuron.2021.09.021
22. Lynch, G., Okubo, T., Hanuschkin, A., Hahnloser, R., Fee, M.: Rhythmic continuous-time coding in the songbird analog of vocal motor cortex. Neuron (2016). https://doi.org/10.1016/j.neuron.2016.04.021
23. Brette, R., Gerstner, W.: Adaptive exponential integrate-and-fire model as an effective description of neuronal activity. J. Neurophysiol. 94 (2005)
24. Fehér, O., Wang, H., Saar, S., Mitra, P.P., Tchernichovski, O.: De novo establishment of wild-type song culture in the zebra finch. Nature (2009). https://doi.org/10.1038/nature07994
25. Araki, M., Bandi, M.M., Yazaki-Sugiyama, Y.: Mind the gap: Neural coding of species identity in birdsong prosody. Science (2016). https://doi.org/10.1126/science.aah6799
26. Prather, J., Peters, S., Nowicki, S., Mooney, R.: Precise auditory-vocal mirroring in neurons for learned vocal communication. Nature (2008). https://doi.org/10.1038/nature06492
27. Prather, J., Okanoya, K., Bolhuis, J.: Brains for birds and babies: Neural parallels between birdsong and speech acquisition. Neurosci Biobehav Rev. (2017). https://doi.org/10.1016/j.neubiorev.2016.12.035